JTTEE5 13:515-520
DOI: 10.1361/10599630421424
1059-9630/$19.00 © ASM International

Diffusion and Phase Transformation on Interface Between Substrate and NiCrAlY in Y-PSZ Thermal Barrier Coatings

Hexing Chen, Kesong Zhou, Zhanpeng Jin, and Chunlei Liu

(Submitted June 17, 2003; in revised form October 3, 2003)

NiCrAlY/Y_2O_3-Y-PSZ (yttria-partially stabilized zirconia) thermal barrier coatings were developed on a superalloy (Ni-10Co-9Cr-7W-5Al, wt.%) surface. The superalloys were first coated with a bond coat of Ni-19Cr-8Al-0.5Y (wt.%) alloy that was deposited by low-pressure plasma spraying and then covered with a top coat of ZrO_2-8wt.%Y_2O_3 by air plasma spraying. The microstructure near the interface was analyzed using an optical microscope, a scanning electron microscope, microhardness measurements, and x-ray diffraction, and the phases of composition were measured using an electron probe microanalyzer after exposure at 1100 °C for different times in air or a vacuum. The reaction processes also were simulated using diffusion-controlled transformation (DICTRA) software in which diffusion was considered as being only the γ phase, and the γ′ phase was treated as spheroidal particles in γ. From the authors' results, it can be concluded that a γ′-phase layer is observed at the interface between substrate and bond coat, and its thickness increases with increasing exposure times in air at 1100 °C. This layer showed good cohesion with the substrate and bond coat. It can also be concluded that the formation of the γ′-phase layer can be predicted from DICTRA simulation. The simulation also shows the same trend of the composition profiles as experimental data.

Keywords: diffusion-controlled transformation, interface reaction, low-pressure plasma spraying, Ni-Cr-Al-Y, thermal barrier coatings

1. Introduction

A plasma-sprayed thermal barrier coating (TBC) system, consisting of an insulating ceramic top coat and an oxidation-resistant metallic bond coat, has been extensively used for the protection of superalloys that are serviced at high temperatures, such as in turbine blades (Ref 1, 2). This allows an increase in operating temperature or an increase in the service intervals of protected parts and therefore reduces the overall operating costs (Ref 3-5).

Sintering and phase transformation can occur in the ceramic deposits of TBCs at high temperatures, and a diffusion reaction can also take place between different coatings, which would cause microstructure changes, form new phases, and even form cracks due to the different expansion rates within the different layers (Ref 6).

Engström et al. (Ref 7-9) developed the method of diffusion simulation. Campbell et al. (Ref 10) established a thermodynamics and kinetics database. These processes involve multiple phases and are difficult to deal with using theoretical models. Attempts have been made to simplify these processes and then use ternary diffusion couples to simulate the diffusion processes (Ref 9, 11). The purpose of this study was to experimentally investigate interface microstructure, phase transformation, and diffusion between the superalloy substrate and the bond coat in TBCs, and then to simulate these processes based on diffusion.

H. Chen, Z. Jin, and **C. Liu,** Department of Materials Science and Engineering, Central South University, Changsha, China; and **K. Zhou,** Guangzhou Research Institute of Non-ferrous Metals, Guangzhou, China. Contact e-mail: chx@mail.gzrinm.com.

2. Experimental Procedures

The substrates used in this study were 10 by 10 by 5 mm samples of DZ125 superalloys (Ni-10Co-9Cr-7W-5Al, wt.%), which were sand-blasted (Al_2O_3, 120 mesh, 0.6 MPa) and then degreased by alcohol and ultrasonic wave treatment. The substrates were first coated with a 160 μm thick NiCrAlY (Ni-19Cr-8Al-0.5Y, wt.%) alloy that was deposited by low-pressure plasma spraying (LPPS). These samples then were covered with a 350 μm thick yttria-stabilized zirconia (YSZ) layer by air plasma spray (APS). The YSZ powders with particle sizes between 40 and

Table 1 Spray parameters

Parameters	YSZ	NiCrAlY
Power, kW	35	42
I, A	500	600
V, V	70	70
Ar flow, L/min	46	46
H_2 flow, L/min	4	6.5
Carrier (Ar) flow, L/min	3	3
Feed rate, g/min	24	22
Spray distance, cm	26	13

I, electric current; V, voltage

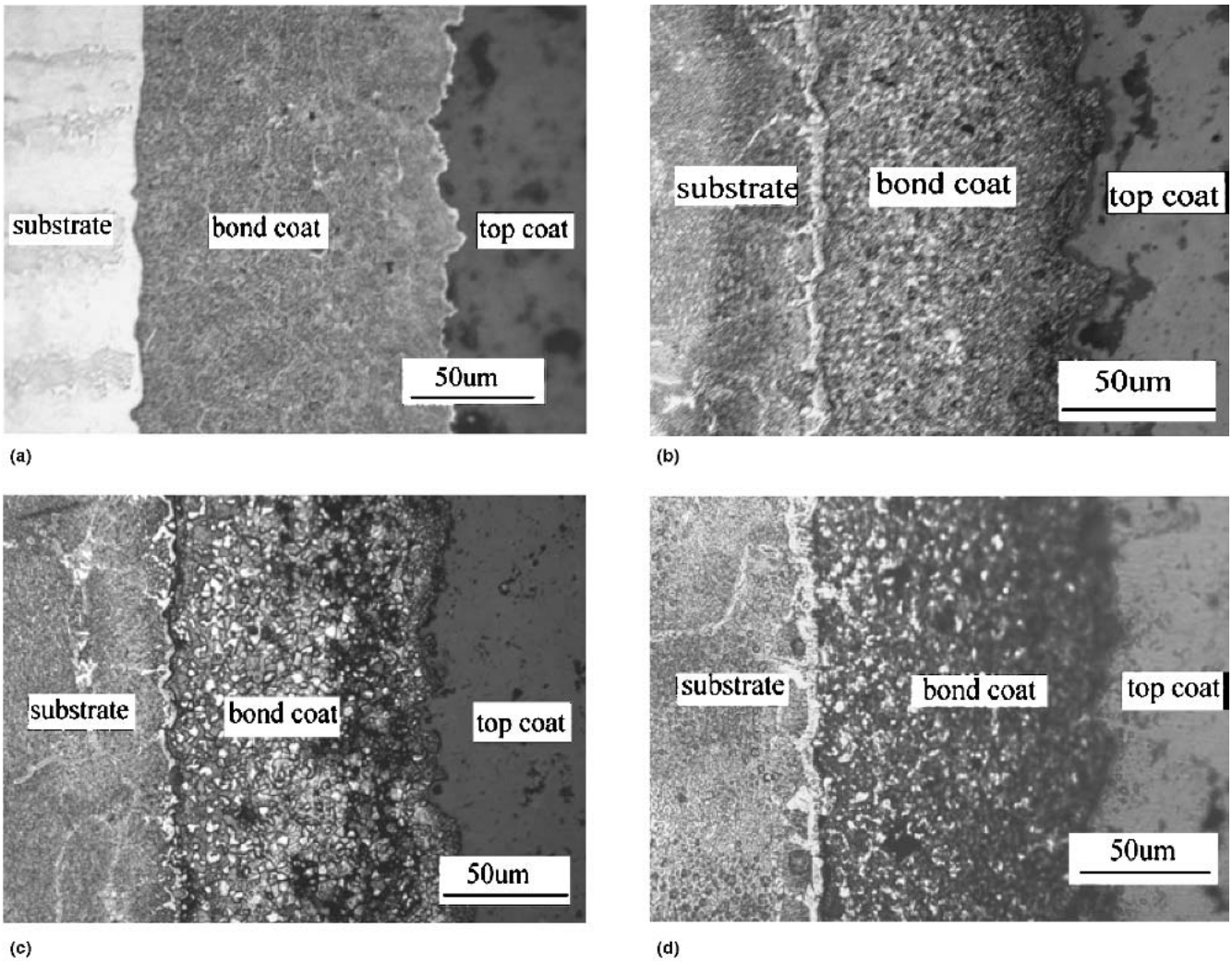

Fig. 1 Optical micrographs along the cross sections of samples exposed at 1100 °C for different times in air or in a vacuum. (a) As sprayed. (b) Exposed for 50 h in air. (c) Exposed for 50 h in vacuum. (d) Exposed for 100 h in air

65 μm contained 8 wt.% yttria (ZrO_2-$8Y_2O_3$). The spray conditions are listed in Table 1.

The specimens were exposed at 1100 °C in air or vacuum for 25, 50, and 100 h, respectively. The microstructure was examined using optical microscopy and a scanning electron microscope (SEM) (JSM-5910, JEOL, Tokyo, Japan). Chemical microanalysis was performed by energy-dispersive spectroscopy (EDS). The phases were analyzed using x-ray diffraction (XRD). Microhardness was also measured.

3. Results and Discussion

3.1 Microstructure and Phase Transformation Near the Substrate/Bond-Coat Interface

The microstructure along the cross section of the samples after spraying and after being exposed at 1100 °C for different times in air or a vacuum is presented in Fig. 1.

Figure 1(b) to (d) shows multiphase structures in the substrate and bond coat. A white layer was formed between the substrate and the bond coat. The thickness of this layer increased with exposure time at 1100 °C. From Fig. 1 white particles (or grains) can be seen in the substrate and bond coat, and their amount increased with increasing exposure time at 1100 °C.

Figure 2 shows the SEM images that reveal the microstructure near the interface between the substrate and the bond coat after different exposure times at 1100 °C in air. A layer was observed at the interface between substrate and bond coat in the SEM images. This layer shows good cohesion with the substrate and bond coat. The microstructures of the substrate and bond coat mainly include both a gray phase (Fig. 2c, B) and a dark gray phase (Fig. 2c, A). The compositions of these phases and the layer were measured by EDS, and the results for the sample that was exposed at 1100 °C for 50 h in air (Fig. 2c) are listed in Table 2. Microhardness data are also given in Table 2. These results indicate that the composition of the precipitated layer is close to the compositions of the dark gray phases in the substrate

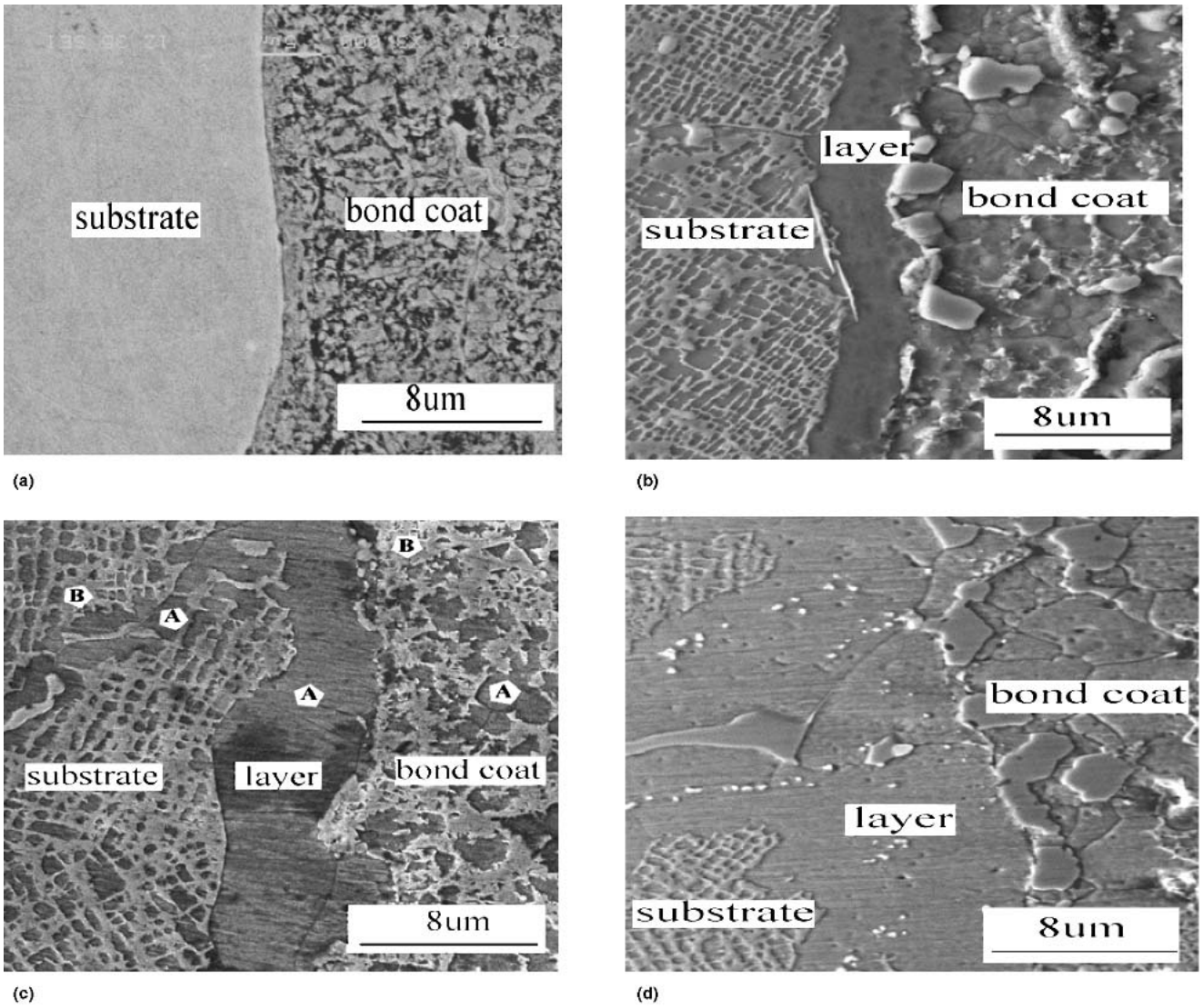

Fig. 2 Microstructure near the substrate/bond-coat interface during different exposed times in air at 1100 °C (SEM photographs). (a) As spraying. (b) Exposed for 25 h in air. (c) Exposed for 50 h in air. (d) Exposed for 100 h in air

and bond coat. The contents of the elements nickel and aluminum in the precipitated layer and in the dark gray phase of the substrate and bond coat are higher than those in the gray phase. The results also indicated that the microhardness of the separate layer (493) was close to that of the dark gray phase in the bond coat (481) and in the substrate (466), but was lower than that of the gray phase in the bond coat (558) and in the substrate (554).

Figure 3 is the distribution of elements nickel, aluminum, and chromium in the sample that was exposed at 1100 °C in air for 100 h. It shows higher contents of nickel and alumium, and a lower content of chromium in the separate layer and the dark gray phases than that in the gray phases. This is consistent with the EDS measurements given in Table 2. The XRD spectra along the cross section of the sample exposed for 100 h in air at 1100 °C are presented in Fig. 4, and they are indexed as γ, γ', and ZrO_2. It is noted that the XRD patterns of the γ phase and γ' phase almost coincide because their crystal lattice constants are close to each other.

Table 2 Composition (at.%) and microhardness of some phases in the sample exposed for 50 h at 1100 °C in air

Variables	GS	DS	SL	GB	DB
Ni	60.4	65.6	67.8	63.2	67.4
Cr	13.2	7.4	6.5	22.2	10.0
Co	10.8	6.9	2.1	3.3	2.4
Al	11.5	18.3	22.5	11.3	20.0
W	3.2	…	…	…	…
Mo	…	0.6	…	…	…
Ti	1.0	…	1.1	…	0.3
Hv					
A	575	480	480	576	503
B	543	459	508	566	459
C	543	459	490	533	480
Hv average	554	466	493	558	481

GS, gray phase in substrate; DS, dark gray phase in substrate; SL, separate layer; GB, gray phase in bond coat; DB, dark gray phase in bond coat. Microanalysis parameters: Accelerating voltage, 15 kV; resolution, 256 × 256; pixel size, 0.140625 μm; Hv, microhardness kgf/mm^2 load, 25 g; time of load, 15 s; Hv average = (A + B + C)/3

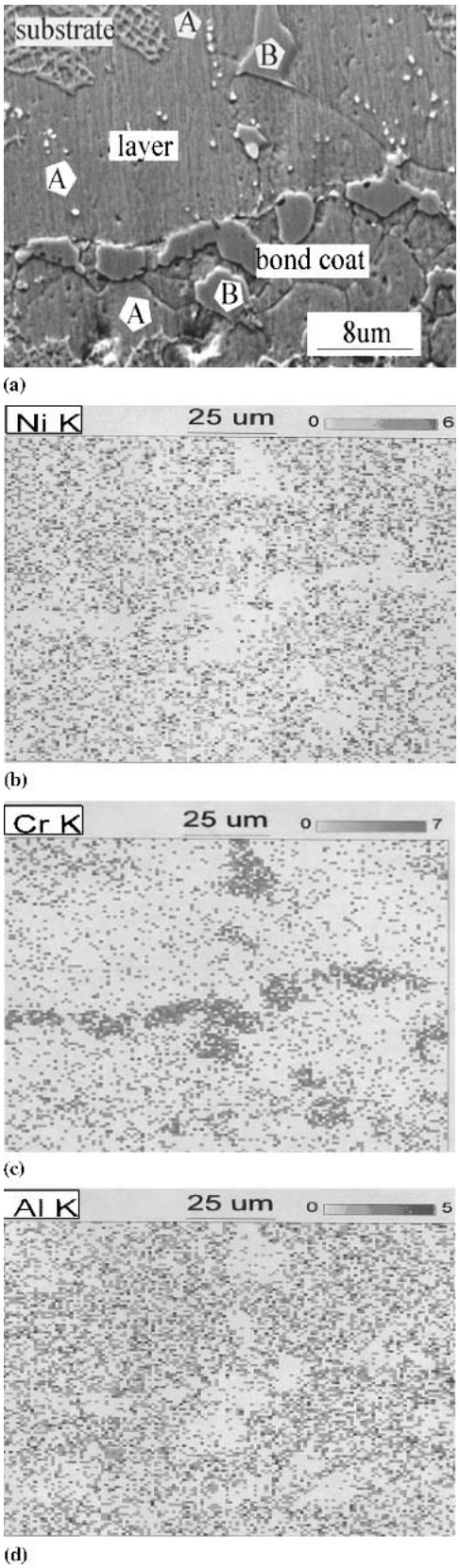

Fig. 3 The distribution of the elements nickel, chromium, and aluminum in the sample exposed at 1100 °C for 100 h in air (a) SEM photograph, (b) Ni, (c) Cr, and (d) Al

Based on the above results, it was concluded that the dark gray phase is the γ' phase and the gray phase is the γ-solution phase. The phase of the separate layer is also the γ' phase because its composition, microhardness, and morphology are similar to those of the dark gray phase in the substrate.

3.2 Simulation and Discussion

An attempt was made in the present work to simulate the reaction processes using diffusion-controlled transformation (DICTRA). Due to a lack of diffusion data in the γ' phase (A_3B intermetallic compound, A is mainly nickel and B is mainly aluminum), the authors considered only the diffusion in the solution phase γ. In the simulation, the γ' phase was assumed to be dispersed phases in spheroidal form, as was investigated in previous work (Ref 8, 9). The authors started the simulation with nickel, chromium, and aluminum, and then added more elements one by one. The final simulation included all elements in the substrate and bond coat. Initially, the substrate consisted of 0.73072 γ + 0.26928 γ', and the bond coat consisted of 0.7957 γ + 0.2043 γ', according to the equilibrium calculation at 1100 °C.

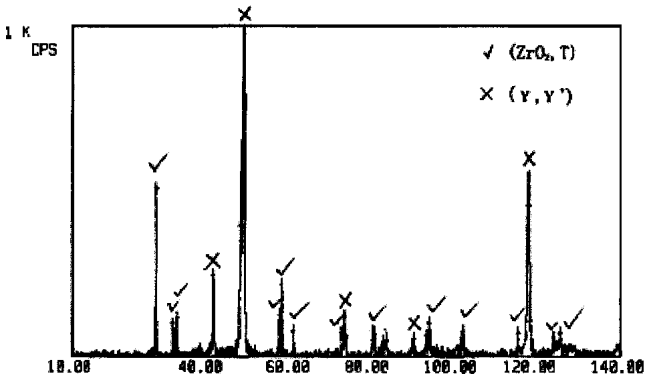

Fig. 4 XRD pattern of the cross section of the sample exposed for 100 h in air at 1100 °C

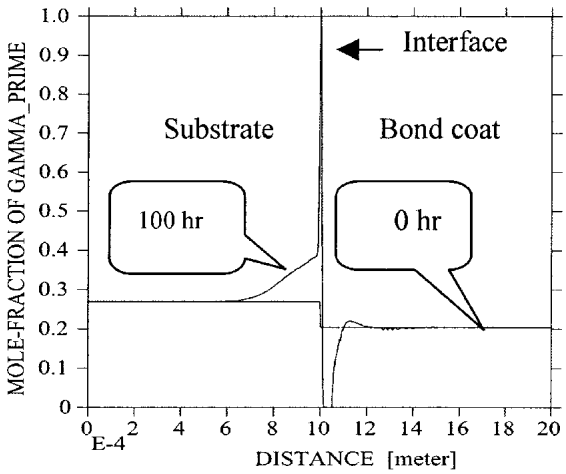

Fig. 5 Fraction of the γ'-phase after being exposed for 100 h in air at 1100 °C according to the DICTRA simulation

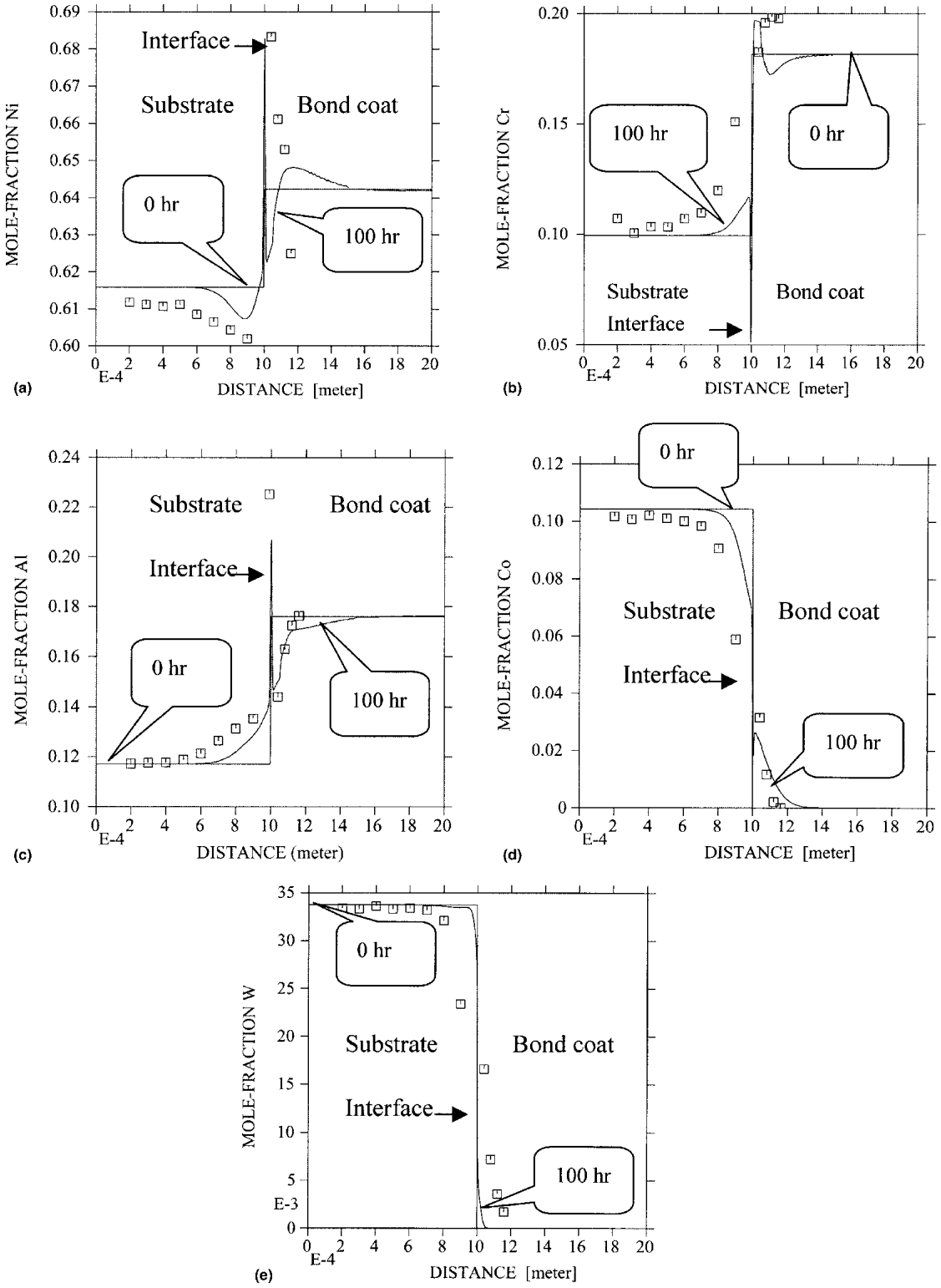

Fig. 6 Composition profiles in the sample exposed at 1100 °C for 100 h according to the DICTRA simulation and experimental data. (a) Nickel. (b) Chromium. (c) Aluminum. (d) Cobalt. (e) Tungsten

The simulation indicated that the γ′ phase formed between the substrate and bond coat after being exposed for 100 h in air at 1100 °C, which is shown in Fig. 5. From Fig. 5, it also can be seen that the γ′ phase grows toward the substrate, which leads to a small amount of γ′ near the bond coat. This is consistent with the authors' experimental observations.

The composition profiles from the DICTRA simulation are presented in Fig. 6 and were compared with the experimental data that were measured as being the average composition in the present work. From these figures, it can be seen that the simulation shows the same trend as the experimental composition profiles, although there are some differences. It is very encouraging that the fraction of the γ' phase and the composition profile near the interface between the substrate and the bond coat can be predicted by using the Thermo-calc and DICTRA software packages if thermodynamics and kinetics databases are available.

4. Conclusions

The interface reaction between the nickel-base superalloy (Ni-10Co-9Cr-7W-5Al, wt.%) and the bond coat exposed at 1100 °C for different times was investigated. The TBCs used in the present work consisted of a bond coat (Ni-19Cr-8.7Al-0.5Y, wt.%) and a top coat (ZrO_2-8wt.%Y_2O_3), and were prepared by LPPS and APS, respectively. The microstructure near the interface was analyzed using optical microscopy, SEM, microhardness, measurements, and x-ray diffraction, and the compositions of the phases were measured using an electron probe microanalyzer. The reaction processes, in which diffusion was considered only as the γ phase and the γ' phase was treated as dispersed and spheroidal particles in the γ phase, were also simulated using DICTRA. From these results, it can be concluded that:

- A γ'-phase layer was observed at the substrate/bond-coat interface, and its thickness increased with increasing exposure time in air at 1100 °C. This layer shows good cohesion with the substrate and bond coat.
- The formation of the γ'-phase layer can be predicted from DICTRA simulation. The simulation also shows the same trend in the composition profiles as the experimental data.

Acknowledgment

The authors would like to thank Dr. Caian Qiu, Questek Systems (Toronto, ON, Canada), for his kind help and instruction. This project (No. 58771037) was supported by the National Natural Science Foundation of China.

References

1. Y. Liu, C. Persson, P. Bengtsson, A.C. Leger, and J. Wigren, Thermal Shock Testing and Finite Element Modeling of Pre-oxidized Thermal Barrier Coatings, *Thermal Spray: Surface Engineering via Applied Research,* C.C. Berndt, Ed., May 8-11, 2000 (Montréal, Québec, Canada), ASM International, 2000, p 173-180
2. J. Wigren and L. Pejryd, Thermal Barrier Coatings: Why, How, Where and Where To, *Thermal Spray: Meeting the Challenges of the 21st Century,* C. Coddet, Ed., May 25-29, 1998 (Nice, France), ASM International, 1998, p 1531-1542
3. R.A. Miller, Current Status of Thermal Barrier Coatings: An Overview, *Surf. Coat. Technol.,* Vol 30, 1987, p 1-11
4. S.M. Meier and D.K. Gupta, The Evolution of Thermal Barrier Coatings in Gas Turbine Applications, *J. Eng. Gas Turbines,* Vol 116 (No. 1), 1994, p 250-257
5. I. Kvernes, E. Lugscheider, and F. Ladru, "Thermal Barrier Coatings in Internal Combustion Engines," presented at Interfacial Engineering of Materials, II Cioceo, Toscana, Italy, Oct 9-14, 1996
6. C.C. Berndt and H. Herman, Failure During Thermal Cycling of Plasma-Sprayed Thermal Barrier Coatings, *Thin Solid Films,* Vol 108, 1983, p 427-437
7. A. Engström, J.E. Morral, and J. Ågren, DICTRA, a Tool for Simulation of Diffusional Transformations in Alloys, *J. Phase Equilib.,* Vol 21 (No. 3), 2000, p 269-280
8. A. Engström, J.E. Morral, and J. Ågren, Computer Simulation of Diffusion in Multiphase Systems, *Metall. Mater. Trans.,* Vol 25A, 1994, p 1127-1134
9. A. Engström, J.E. Morral, and J. Ågren, Computer Simulations of Ni-Cr-Al Multiphase Diffusion Couples, *Acta Mater.,* Vol 45, 1997, p 1189-1199
10. C.E. Campbell, W.J. Boettinger, and U.R. Kattner, Development of a Diffusion Mobility Database for Ni-Base Superalloys, *Acta Mater.,* Vol 50, 2002, p 775-792
11. A. Engström, Interdiffusion in Multiphase, Fe-Cr-Ni Diffusion Couples, *Scand. J. Metall.,* Vol 24, 1995, p 12-20